Contribution from the Department of Chemistry,
Purdue University, West Lafayette, Indiana 47907-3699

Evidence for Dissociative Photosubstitution Reactions of $[Ru(trpy)(bpy)(NCCH_3)]^{2+}$. Crystal and Molecular Structure of $[Ru(trpy)(bpy)(py)](PF_6)_2 \cdot (CH_3)_2CO$

Clark R. Hecker, Phillip E. Fanwick, and David R. McMillin*

Received September 13, 1990

In acetonitrile and in the presence of appropriate nucleophiles, the complex $[Ru(trpy)(bpy)(NCCH_3)]^{2+}$ undergoes a ligand substitution reaction when irradiated into the metal-to-ligand absorption band system. (The symbol trpy denotes 2,2':6',2''-terpyridine, and bpy denotes 2,2'-bipyridine.) At 25 °C quantum yields for displacement of the acetonitrile ligand are 0.0013 (1), 0.0013 (1), and 0.0026 (5) for 1.0 M solutions of pyridine, 4-phenylpyridine, and 2-methylpyridine, respectively. No photochemistry is observed for the osmium(II) analogue, and all findings can be understood in terms of a dissociative reaction mechanism involving a reactive ^{3}d-d state. The ^{3}d-d state is accessed from a ^{3}CT state, which is emissive below ca. 180 K. From measurements of the temperature dependence of the emission lifetime, the barrier to population of the ^{3}d-d state is approximately 1500 cm^{-1}. Finally, the crystal structure of $[Ru(trpy)(bpy)(py)](PF_6)_2 \cdot (CH_3)_2CO$ has been determined with a diffractometer. The compound crystallizes with two independent formula units in a triclinic unit cell. The space group is $P\bar{1}$, and there are four formulas per unit cell ($Z = 4$) with $a = 13.150$ (1) Å, $b = 14.927$ (1) Å, $c = 19.771$ (2) Å, $\alpha = 102.840$ (9)°, $\beta = 91.655$ (8)°, and $\gamma = 103.371$ (8)°. The structure was solved by the full-matrix least-squares method, and after the final stage of refinement, $R = 0.055$. There is evidence of interligand steric strain within the coordination sphere, and the bpy ligand is coordinated asymmetrically with a difference in Ru-N bond lengths of about 0.04 Å. The internal strain probably explains why we have been unable to prepare the 2-methylpyridine analogue by standard methods.

Introduction

Complexes of ruthenium(II) with polypyridyl ligands have been intensely studied because of the diverse variety of excited-state phenomena that have been observed, including photoluminescence, chemiluminescence, photoredox chemistry, and photosubstitution processes.[1-4] The luminescent excited state is usually a metal-to-ligand charge-transfer (CT) state with triplet multiplicity. On the other hand, photosubstitution is generally assumed to occur via a dissociative mechanism involving a thermally accessible ligand field excited state with triplet multiplicity, i.e., a ^{3}d-d state.[5-8] Recently, however, Tachiyashiki and Mizumachi have suggested that the mechanism of photoanation of $Ru(bpy)_3^{2+}$ has associative character in aqueous acid solution[9] where, as usual, bpy denotes 2,2'-bipyridine. In addition, certain d^6 complexes of tungsten(0) have been shown to have ^{3}CT states of the metal-to-ligand type that undergo associative substitution reactions.[10] Associative processes are feasible because the increase in the formal charge of the metal center in the CT state makes the metal center a better electrophile.[11]

Unfortunately, the interpretation of much of the photochemical data regarding ruthenium(II) polypyridine systems is complicated by that fact competing processes are usually evident. For example, the first step in the photoanation of $Ru(bpy)_3^{2+}$ occurs when an anion intercepts an intermediate with a bpy group coordinated in an η^1 fashion. At this point another anion can attack to give product, or rechelation of the η^1 bpy can occur with expulsion of the anion. The branching ratio clearly influences the overall yield. In studies of $Ru(NN)_2L_2^{2+}$ systems, where NN denotes a bidentate, heteroaromatic ligand such as bpy and L is a monodentate ligand, the photochemistry is also complicated because it involves the sequential loss of two L groups. The photoanation yield is enhanced in weakly polar solvents like CH_2Cl_2[12,13] due to ion pairing, but the equilibrium constants for ion pair formation vary with the anion. Another pitfall associated with weakly donating solvents is that the primary photoproduct may be a solvento complex that subsequently undergoes anation.[14]

In an attempt to minimize these difficulties, we have embarked on studies of $[Ru(trpy)(bpy)(NCCH_3)]^{2+}$ where trpy denotes the tridentate ligand 2,2':6',2''-terpyridine. This complex is useful because it is thermally inert and because acetonitrile is a good, unidentate leaving group. Thus, we usually observe only one net photoproduct. Furthermore, the photochemistry has been investigated in acetonitrile to minimize the complications associated with formation of a solvent adduct during the substitution reaction. Three neutral pyridine (py) ligands with varying stereoelectronic properties have been used as entering groups, and the results provide strong support for the notion that photosubstitution occurs by a dissociative mechanism. As a further means of characterizing the system, we have also solved the crystal and molecular structure of $[Ru(trpy)(bpy)(py)](PF_6)_2 \cdot (CH_3)_2CO$. Finally, in attempt to determine the barrier separating the ^{3}CT and ^{3}d-d excited states of the precursor, we have measured the emission lifetime over a range of temperatures.

Experimental Section

Materials. Starting materials and other reagents including $RuCl_3 \cdot nH_2O$, K_2OsCl_6, KPF_6, $AgPF_6$, $AgNO_3$, pyridine, 2-methylpyridine (2-Me-py), and poly(methyl methacrylate) were obtained as reagent grade materials from standard commercial suppliers. Most were used without further purification except that pyridine and 2-picoline were distilled from Na or KOH prior to use in the photolysis experiments. 4-Phenylpyridine (4-Ph-py) was obtained from Aldrich and was sublimed twice before use.

The trpy and bpy ligands were also obtained from Aldrich as were the solvents propionitrile and butyronitrile. The latter two solvents were distilled from P_4O_{10} under nitrogen and stored under a dry, inert atmosphere. Acetonitrile was obtained from Burdick & Jackson or Mallinckrodt while CH_2Cl_2 was from Burdick & Jackson. $AgNO_2$ was prepared by metathesis from $NaNO_2$ and $AgNO_3$ in cold aqueous solution. $K_3[Fe(C_2O_4)_3]$ was prepared by a literature method.[15] The synthetic intermediate $[Ru(trpy)(bpy)Cl]PF_6$ was prepared by the method of Calvert et al.[16] The $[Os(trpy)(bpy)Cl]PF_6$ was prepared by the

* Author to whom correspondence should be addressed.

(1) Kalyanasundaram, K. *Coord. Chem. Rev.* **1982**, *46*, 159-244.
(2) Balzani, V.; Bolletta, F.; Gandolfi, M. T.; Maestri, M. *Top. Curr. Chem.* **1978**, *75*, 1-64.
(3) Krausz, E.; Ferguson, J. *Prog. Inorg. Chem.* **1989**, *37*, 293-390.
(4) Hoffman, M. Z.; Bolletta, F.; Moggi, L.; Hug, G. L. *J. Phys. Chem. Ref. Data* **1989**, *18*, 219-543.
(5) van Houten, J.; Watts, R. J. *Inorg. Chem.* **1978**, *17*, 3381-3385.
(6) Xu, J.; Porter, G. B. *Can. J. Chem.* **1982**, *60*, 2856-2858.
(7) Durham, B.; Caspar, J. V.; Nagle, J. K.; Meyer, T. J. *J. Am. Chem. Soc.* **1982**, *104*, 4803-4810.
(8) Ross, H. B.; Boldaji, M.; Rillema, D. P.; Blanton, C. B.; White, R. P. *Inorg. Chem.* **1989**, *28*, 1013-1021.
(9) Tachiyashiki, S.; Mizumachi, K. *Chem. Lett.* **1989**, 1153-1154.
(10) van Dijk, H. K.; Servaas, P. C.; Stufkens, D. J.; Oskam, A. *Inorg. Chim. Acta* **1986**, *104*, 179-183.
(11) McMillin, D. R.; Kirchhoff, J. R.; Goodwin, K. V. *Coord. Chem. Rev.* **1985**, *64*, 83-92.
(12) Hoggard, P. E.; Porter, G. B. *J. Am. Chem. Soc.* **1978**, *100*, 1457-1463.
(13) Durham, B.; Walsh, J. L.; Carter, C. L.; Meyer, T. J. *Inorg. Chem.* **1980**, *19*, 860-865.
(14) Milder, S. J.; Gray, H. B.; Miskowski, V. M. *J. Am. Chem. Soc.* **1984**, *106*, 3764-3767.
(15) Hatchard, C. G.; Parker, C. A. *Proc. R. Soc. London, A* **1956**, *235*, 518-536.
(16) Calvert, J. M.; Schmehl, R. H.; Sullivan, B. P.; Facci, J. S.; Meyer, T. J.; Murray, R. W. *Inorg. Chem.* **1983**, 2151-2162.

0020-1669/91/1330-0659$02.50/0

method of Dwyer and co-workers.[17]

[Ru(trpy)(bpy)(py)](PF$_6$)$_2$. Into a 250-mL round-bottom flask were placed 0.231 g of [Ru(trpy)(bpy)Cl]PF$_6$, 0.5 mL of pyridine, 35 mL of water, and 35 mL of ethanol. The solution was refluxed with stirring for 5 h, and the color changed from maroon to brown. The volume was then reduced by half with rotary evaporation, and a few milliliters of saturated aqueous KPF_6 solution was added. The precipitate was collected by suction filtration, washed twice with ether, and air-dried. The crude product was eluted from Brockmann Grade III acidic alumina with 2:1 toluene/CH_3CN, and the main brown band was collected. After the solvents were removed by rotary evaporation, the brown powdery residue was redissolved in acetone and precipitated with ether. It was then collected by suction filtration, washed with ether, and air-dried. Yield: 0.0875 g (30%). Anal. Calcd: C, 41.92; N, 9.78; H, 2.81. Found: C, 41.72; N, 9.59; H, 3.06. Crystals suitable for structure determination were obtained from evaporation of a solution of the compound in a mixture of toluene, acetone, and a small amount of pyridine. The supernatant was removed, and the deep orange-red needles were washed with pentane and air-dried.

[Ru(trpy)(bpy)NO$_2$]PF$_6$. A 250-mL round-bottom flask was charged with 100 mL of water, 20 mL of acetone, 0.574 g of [Ru(trpy)(bpy)Cl]PF$_6$, and 0.155 g of $AgNO_2$. The solution was heated at reflux and stirred for 2 h, whereupon it changed from maroon to orange. The solution was filtered while hot, and the solvent was removed with a rotary evaporator. The dull orange powder which was obtained was redissolved in acetone and precipitated with ether. Then it was collected by suction filtration, washed with ether, and air-dried. Yield: 0.343 g (59%).

[Ru(trpy)(bpy)NO](PF$_6$)$_3$. To a suspension of 0.231 g of [Ru(trpy)(bpy)NO$_2$]PF$_6$ in 60 mL of methanol were added 7 mL of concentrated HPF_6. After 20 min, the product formed as an insoluble, yellow powder, which was collected by suction filtration and washed with water, ethanol, and ether, before it was dried in air. Yield: 0.283 g (88%).

[Ru(trpy)(bpy)(NCCH$_3$)](PF$_6$)$_2$. A 0.2-g sample of [Ru(trpy)(bpy)NO](PF$_6$)$_3$ was suspended in 20 mL of CH_3CN with gentle stirring. Solid NaN_3 was added slowly, and a small amount of gas (presumably N_2 and N_2O) bubbled from the bed of NaN_3 for ca. 45 min. When gas evolution ceased, the solution was decanted, and the solvent was removed with a rotary evaporator. The product was then eluted from alumina as described above, and the supernatant solvent was removed by rotary evaporation. The product was recrystallized from a CH_3CN/toluene mixture, and the red prisms were washed with pentane and air-dried. Anal. Calcd: C, 39.47; N, 10.23; P, 7.54; H, 2.70. Found: C, 39.61; N, 10.19; P, 7.85; H, 2.70.

[Ru(trpy)(bpy)(4-Ph-py)](PF$_6$)$_2$. A small amount of [Ru(trpy)(bpy)NO](PF$_6$)$_3$ was added to a solution of 4-phenylpyridine in ethanol. Solid NaN_3 was added, and the solution was stirred gently until gas evolution ceased. The liquid portion was then decanted and reduced to dryness with a rotary evaporator. The product was redissolved in an acetone/toluene mixture and deposited as a dark red, glassy solid as the solvent evaporated.

[Ru(trpy)(bpy)(2-Me-py)](PF$_6$)$_2$. Repeated attempts to produce this species in 2-picoline solution by a method similar to the above resulted only in impure product. Apparently this complex is quite labile and subject to rapid substitution with water on exposure to moist air. Other modes of decomposition are also possible.

[Os(trpy)(bpy)(NCCH$_3$)](PF$_6$)$_2$. A 0.035-g sample of [Os(trpy)(bpy)Cl]PF$_6$ in a 50-mL round-bottom flask was dissolved in a 7:3 mixture of ethylene glycol and CH_3CN. The solution was heated at reflux for 3 days and periodically replenished with CH_3CN. The reaction was halted after the solution changed from green to greenish brown. The resulting mixture was loaded onto an alumina column equilibrated with 2:1 toluene/CH_3CN and eluted with the same solvent. The brown band was recovered, and the solvent was removed by rotary evaporation. The crude product was dissolved in acetone, precipitated with ether, collected by suction filtration, and dried in air. Finally, the product was reprecipitated as a dark brown powder from CH_2Cl_2.

Equipment. Infrared spectra were obtained on a Perkin-Elmer FTIR instrument with KBr disks. UV/visible spectra were obtained on a Perkin-Elmer Lambda 4C spectrophotometer fitted with a thermocouple-driven temperature controller set to 25 °C. A Vacuum Atmospheres HE-43-2 drybox filled with nitrogen was used for solvent storage. The X-ray structure was determined with an Enraf-Nonius CAD4 computer-controlled κ-axis diffractometer equipped with a graphite crystal incident-beam monochromator.

Photochemistry. Irradiations were performed with an Oriel Model 66020 arc lamp equipped with a Hanovia 976C0010 1-kW Xe lamp element and an Oriel Model 8540 power supply. The collimated beam was directed through a water filter and focused on an Oriel 7540 monochromator set at 464 nm. A small portion of the monochromatic beam was reflected off a quartz plate to a photodiode interfaced to an X-Y recorder in time-base mode to monitor lamp stability. The balance of the beam intensity passed on to a water-jacketed cuvette holder whose temperature was controlled at 25 °C with a Tri-R B-30 methanol/water bath set at 25 °C. Continuous agitation was provided by a Tri-R MS-7 magnetic stir base driving a 7 or 8 mm Teflon-coated stir bar inside the cuvette.

Luminescence. Samples were thermostated in either an Oxford Instruments DN-1704 liquid-nitrogen cryostat equipped with a solid sample holder and an ITC-4 temperature controller or an Oxford Instruments DN-704 model with a temperature controller constructed by Gary Kramer from this department. Steady-state luminescence spectra were obtained either on a Perkin-Elmer MPF-44B fluorescence spectrophotometer or on an SLM-Aminco SPF-500C instrument. Luminescence lifetimes were obtained with an apparatus that has been described previously.[18]

Photochemical Methodology. Samples were mixed just before photolysis and sealed in glass or quartz precision cuvettes while in the inert-atmosphere box. Stock solutions of CH_3CN, 1.00 M in the appropriate pyridine, were mixed beforehand and kept in sealed flasks. Samples were given three freeze–pump–thaw cycles and resealed under dry nitrogen or argon. Spectral scans were taken over the range 350–700 nm, and solutions were mixed to have a maximum absorbance in the range 1.2–1.9, as measured against a solvent blank. Each of three reaction systems shared an isosbestic point at 464 nm, where the irradiations were carried out. Typical irradiation times ranged from 4 to 9 h total with a light flux of $(1–2) \times 10^{-8}$ einstein s^{-1}. The slits of the excitation monochromator were set at 2 mm. Photochemical conversion was usually in the range 15–45%. Absolute lamp intensity measurements were performed by potassium ferrioxalate actinometry with deoxygenated solutions that were stirred magnetically.

The mathematical equations appropriate for irradiation at an isobestic point have been described.[19] A computer program called SHINE was written in Idris BASIC so that experimental absorbance data over the whole range of wavelengths could be used. The input includes the extinction coefficient of the photoproduct at each wavelength analyzed as well as the experimental difference spectra. The quantum yield of reaction is then estimated by a standard least-squares algorithm based on a comparison of the experimental and calculated difference spectra. In each case, the program QYFIT[20] was also used to analyze the data. This program determines the product spectrum as well as the quantum yield. Good agreement was obtained between the two methods.

Luminescence Methodology. Solution samples were prepared in the drybox and deoxygenated as before. The solid-state samples were prepared by pressing small crystals between two glass plates mounted on the solid sample holder. Samples in a poly(methyl methacrylate), or pmm, host were produced by dissolving the compound and filtering the solution onto beads of the polymer in CH_2Cl_2. The solution was then dripped onto a quartz plate, covered, and allowed to dry in the dark overnight before use. Usable film exhibited a network of fine fractures, but if the solvent evaporated too rapidly, the resulting film developed an unsatisfactory frosted surface. The plate was mounted on the solid sample holder. Data sets usually consisted of 256 points per scan, and four scans were taken per temperature. Lifetime calculations were performed by a standard weighted exponential least-squares fit routine; temperature versus lifetime fitting (single and double exponential) was performed with user-written software.

Crystallography. A crystal of [Ru(trpy)(bpy)(py)](PF$_6$)$_2$·(CH$_3$)$_2$CO with approximate dimensions of $0.3 \times 0.2 \times 0.04$ mm was mounted on a glass fiber. Preliminary examination and data collection were performed with Mo Kα radiation ($\lambda = 0.71073$ Å). Cell constants and an orientation matrix for data collection were determined from the setting angles of 25 reflections in the range of $13° < \theta < 16°$. As a check on crystal quality, ω scans of several intense reflections were measured. The width at half-height was 0.64° with a take-off angle of 3.2°. The data were collected at a temperature of 20 ± 1 °C by using the ω-2θ scan technique. The scan rate varied from 2 to 20°/min (in ω). Data were collected to a maximum 2θ of 45.0°. A total of 9516 reflections, all unique, were collected. The ruthenium atoms were located from the Patterson map; other atoms were subsequently located by means of the

(17) Dwyer, F. P.; Buckingham, D. A. *Aust. J. Chem.* **1964**, *17*, 622–631.

(18) Gamache, R. E., Jr.; Rader, R. A.; McMillin, D. R. *J. Am. Chem. Soc.* **1985**, *107*, 1141–1146.

(19) Kirchhoff, J. R.; McMillin, D. R.; Marnot, P. A.; Sauvage, J. P. *J. Am. Chem. Soc.* **1985**, *107*, 1138–1141.

(20) Stacy, N. E.; McMillin, D. R. *J. Photochem. Photobiol. A* **1989**, *47*, 83–89.

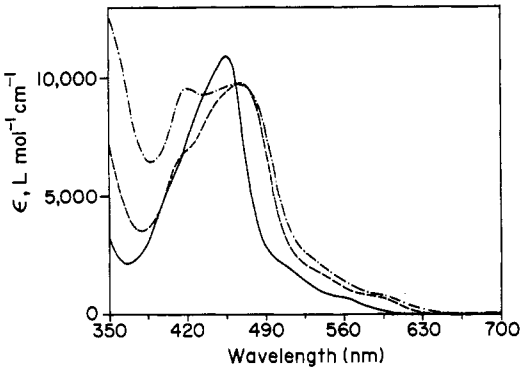

Figure 1. Absorbance spectra of $[Ru(trpy)(bpy)(NCCH_3)]^{2+}$ (—); $[Ru(trpy)(bpy)(py)]^{2+}$ (– –); and $[Ru(trpy)(bpy)(4\text{-}Ph\text{-}py)]^{2+}$ (–·–) in acetonitrile at 25 °C.

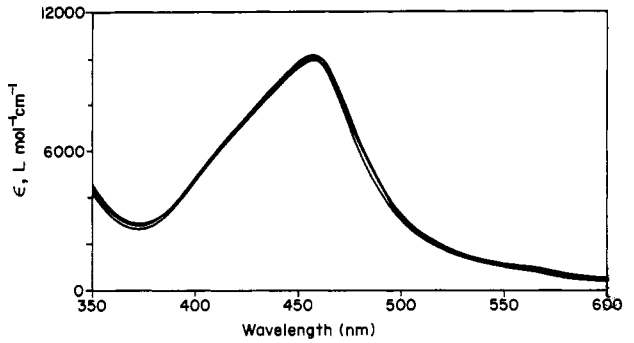

Figure 2. Absorbance spectra of $[Ru(trpy)(bpy)(2\text{-}Me\text{-}py)]^{2+}$ in acetonitrile at 25 °C. Each spectrum was determined with the program QYFIT and a different set of photolysis data.

DIRDIF program. During the solution, positions of hydrogen atoms were included but not refined.

Results

Absorption Spectra. The absorbance spectrum of $[Ru(trpy)(bpy)(NCCH_3)]^{2+}$ exhibits, both in solution and in plastic films, an MLCT transition peaking at 454 nm with an extinction coefficient of 10900 ± 100 L/(mol cm) along with shoulders at about 512 and about 563 nm (Figure 1). The main band undoubtedly includes unresolved excitations from the d shell of ruthenium(II) to the lowest energy π^* orbitals of the trpy and bpy ligands. In the case of $[Ru(tpy)(bpy)(py)]^{2+}$, the spectrum is broadened with a maximum at 467 nm, and there is a prominent shoulder near 415 nm. Weak bands are also evident at 538 and 595 nm (Figure 1). The spectrum of $[Ru(trpy)(bpy)(4\text{-}Ph\text{-}py)]^{2+}$ is similar with an intense band maximizing at 464 nm, but there is a well-resolved maximum at 420 nm along with the shoulders at 546 and at 597 nm (Figure 1). The absorption spectrum of authentic $[Ru(tpy)(bpy)(2\text{-}Me\text{-}py)]^{2+}$ could not be obtained directly, due to our inability to prepare the pure compound. However, a reproducible spectrum was resolved from photolysis data with the program QYFIT (Figure 2). For this derivative the λ_{max} is 457 nm, and there is evidence of a poorly resolved shoulder at around 410 nm.

Photochemistry. When $[Ru(trpy)(bpy)(NCCH_3)]^{2+}$ was irradiated in the presence of a pyridine ligand dissolved in CH_3CN, the CT absorption bands shifted to longer wavelength, and a new band grew in at around 415 nm. Two isosbestic points were always observed, and quantum yields were determined by irradiating at the longer wavelength isosbestic point. Quantum yields are compiled in Table I. Each entry is the average of two trials except for the 2-Me-py datum which is the average of four trials. In each case, the reaction corresponded to the replacement of acetonitrile by a pyridine, and there was no evidence for any other photoreaction. Good agreement between quantum yields was obtained when the data were analyzed by the algorithms employed in the computer program SHINE and QYFIT. The experimental difference spectrum, obtained with 4-Ph-py and the original complex in solution in the reference sample, is presented as a function of time of irradiation in Figure 3.

Table I. Quantum Yields for Photosubstitution of $[Ru(trpy)(bpy)(NCCH_3)]^{2+}$

nucleophile[a]	ϕ
py	0.0013 ± 0.0001
4-Ph-py	0.0012 ± 0.0001
2-Me-py	0.0026 ± 0.0005

[a] 1.0 M solution in acetonitrile at 25 °C.

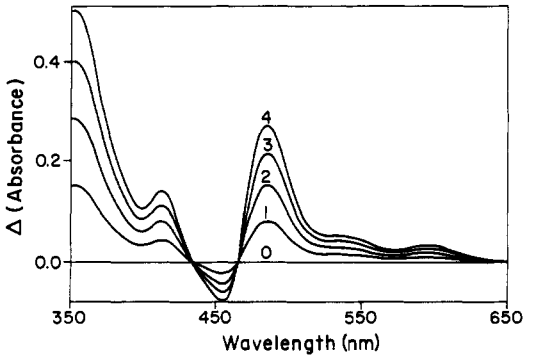

Figure 3. Difference spectra obtained with irradiation of $[Ru(trpy)(bpy)(NCCH_3)]^{2+}$ in acetonitrile containing 1 M 4-Ph-py. The reference spectrum is that of the unirradiated solution, and the concentration of complex was 1.40×10^{-4} M. Irradiation was carried out at a wavelength of 464 nm and at 25 °C. The cumulative time of irradiation is indicated for each spectrum in units of hours.

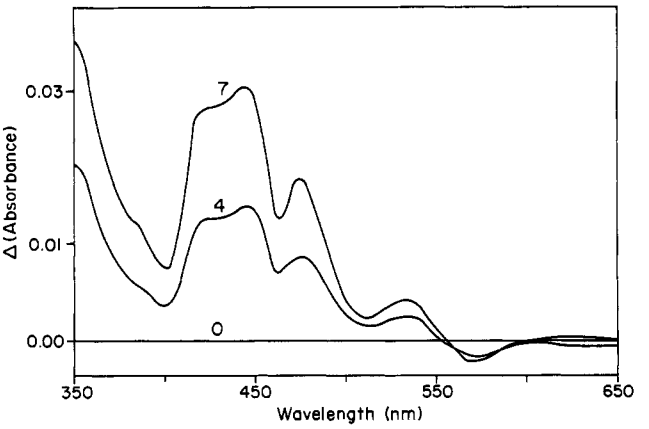

Figure 4. Difference spectra obtained from irradiation of $[Ru(trpy)(bpy)(NCCH_3)]^{2+}$ in acetonitrile containing approximately 1 M bpy. The cumulative time of irradiation is indicated for each spectrum in units of hours, and the conditions were the same as in Figure 3.

Several control studies were also carried out. We checked for evidence of a secondary photoreaction by irradiating a sample of $[Ru(trpy)(bpy)(py)]^{2+}$ in CH_3CN, but there was no indication of any reaction after several hours of irradiation. In view of the difficulties encountered in the preparation of the 2-Me-py derivative, we checked for evidence of a thermal back-reaction after photolysis, but no loss of $[Ru(trpy)(bpy)(2\text{-}Me\text{-}py)]^{2+}$ occurred in situ after incubation for 0.5 h in the dark. We also irradiated $[Os(trpy)(bpy)(NCCH_3)]^{2+}$ in CH_3CN in the presence of 1 M pyridine, and we found no evidence of any net reaction. Qualitative photolysis experiments were also carried out with bpy as a nucleophile. When $[Ru(trpy)(bpy)(NCCH_3)]^{2+}$ was photolyzed in the presence of approximately 1 M bpy, a different type of photoproduct or (photoproduct distribution) appeared to form. As can be seen in Figure 4, the absorbance increased at virtually all wavelengths between 350 and 500 nm.

Luminescence. With the equipment available, essentially no emission could be detected from the CH_3CN complex in solution above 180 K, but it exhibited an orange-red emission at lower temperatures upon illumination into the MLCT or $\pi-\pi^*$ absorption bands. Parameters that can be used to explain the

Table II. Parameters for the Temperature Dependence of Luminescence Decay

complex	k_0, s^{-1}	A_1, s^{-1}	ΔE_1, cm^{-1}	A_2, s^{-1}	ΔE_2, cm^{-1}
		In 5:4 (V/V) C_3H_7CN/C_2H_5CN			
$[Ru(bpy)_3]^{2+}$ [a]	2.3×10^5	1.4×10^{14}	3960	5.6×10^5	90
$[Ru(trpy)(bpy)(NCCH_3)]^{2+}$	1.7×10^5	2.1×10^{14}	1560		
		In Poly(methyl methacrylate)			
$[Ru(trpy)_2]^{2+}$ [b]	1.1×10^5			2.4×10^6	230
$[Ru(trpy)(bpy)(NCCH_3)]^{2+}$	1.2×10^5			3.1×10^6	160
		In the Solid State			
$[Ru(trpy)(bpy)(NCCH_3)](PF_6)_2$	1.5×10^5	2.3×10^{11}	1200	1.3×10^6	160

[a] de Cola, L.; Barigelletti, F.; Cook, M. J. *Helv. Chim. Acta* **1988**, *71*, 733–741. [b] Hecker, C. R.; McMillin, D. R. Unpublished results.

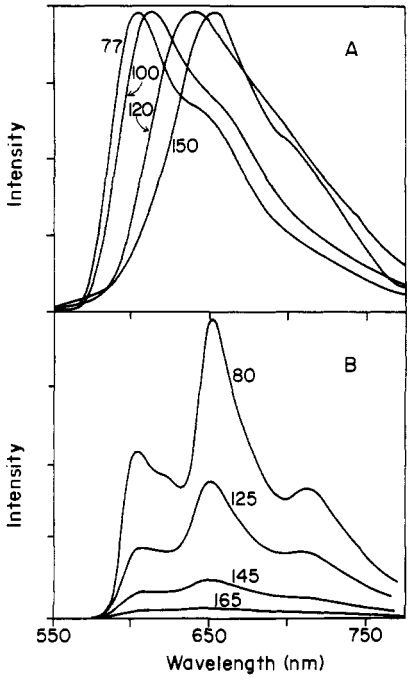

Figure 5. (A) Normalized, corrected emission spectra of $[Ru(trpy)(bpy)(NCCH_3)]^{2+}$ obtained in C_2H_5CN/C_3H_7CN solution as a function of temperature. The temperature is indicated for each spectrum in units of K. (B) Corrected emission spectra measured from solid $[Ru(trpy)(bpy)(NCCH_3)](PF_6)_2 \cdot (CH_3)_2CO$ with the temperature indicated in units of K. In both cases the exciting wavelength was 454 nm.

temperature dependence of the lifetime, vide infra, are presented in Table II.

The shape of the emission spectrum varied with the medium. At low temperatures in 5:4 C_3H_7CN/C_2H_5CN, some evidence of vibronic structure was evident in the emission spectrum with the highest intensity component on the high energy side of the spectrum (Figure 5A). Above 110 K, when the matrix began to soften, the spectrum broadened and shifted to longer wavelength. Despite the fact that the wavelength of the emission maximum shifted in the softened matrix, the luminescence decay conformed to a simple exponential decay. Accordingly, there was no need to resort to the analysis of time-resolved spectra.[21] In a pmm film a broad unstructured emission was observed at all temperatures with the emission maximum at about 600 nm. In the crystalline state a structured emission was observed with the apparent intensity maximum occurring in the second major vibronic component (Figure 5B). The spacing between the three well-resolved vibronic components was ca. 1200 cm^{-1}.

Structure of $[Ru(trpy)(bpy)(py)](PF_6)_2 \cdot (CH_3)_2CO$. Two formula equivalents were found in the asymmetric unit. The crystal data are compiled in Table III. The coordinates of all non-hydrogen atoms are presented in Table IV, and selected bond distances and angles are listed in Table V. In Figure 6, the atom numbering system is illustrated with an ORTEP drawing of one of the complex ions from the asymmetric unit.

Table III. Crystal Data and Collection Parameters for $[Ru(trpy)(bpy)(py)](PF_6)_2 \cdot (CH_3)_2CO$

empirical formula	$RuP_2F_{12}ON_6C_{33}H_{30}$
fw	917.65
space group	$P\bar{1}$
a, Å	13.150 (1)
b, Å	14.927 (1)
c, Å	19.771 (2)
α, deg	102.840 (9)
β, deg	91.655 (8)
γ, deg	103.371 (8)
V, Å^3	3668 (1)
Z	4
d_{calc}, g cm^{-3}	1.662
cryst dimens, mm	0.30 × 0.20 × 0.04
T, °C	20
radiation (wavelength)	Mo Kα (0.710 73 Å)
monochromator	graphite
linear abs coeff, cm^{-1}	6.00
abs cor applied	empirical[a]
transm factors: min; max	0.70; 1.00
diffractometer	Enraf-Nonius CAD4
scan method	ω–2θ
h,k,l limits	−14 to 14, −16 to 15, 0 to 21
2θ range, deg	4.00–45.00
scan width, deg	0.64 + 0.35 tan θ
take-off angle, deg	3.15
programs used	Enraf-Nonius SDP
F_{000}	1840.0
p factor used in weighting	0.060
no. of data collcd	9516
no. of unique data	9516
no. of data with $I > 3.0\sigma_I$	6048
no. of variables	951
largest shift/esd in final cycle	0.76
R	0.055
R_w	0.069
goodness of fit	1.107

[a] Walker, N.; Stewart, D. *Acta Crystallogr.* **1983**, *A39*, 158.

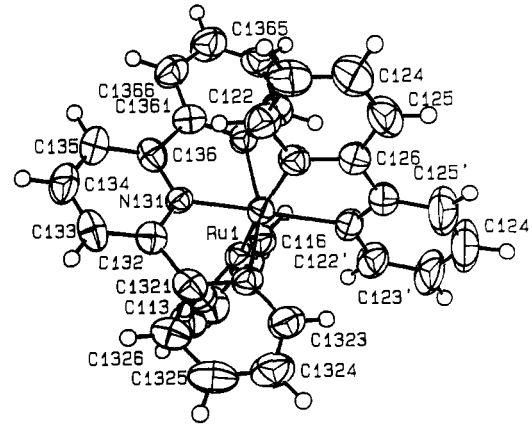

Figure 6. ORTEP drawing of form 1 of the cation $[Ru(trpy)(bpy)(py)]^{2+}$ along with the atom numbering system. Except for the hydrogens, the atom positions are indicated with 50% probability ellipsoids.

(21) Kim, H.-B.; Kitamura, N.; Tazuke, S. *Chem. Phys. Lett.* **1988**, *143*, 77–80.

Table IV. Positional Parameters and Their Estimated Standard Deviations

atom	x	y	z	B, Å²	atom	x	y	z	B, Å²
Ru(1)	0.35221 (5)	0.22827 (4)	0.55034 (3)	3.37 (1)	C(1363)	0.5236 (7)	0.1875 (6)	0.6418 (5)	4.8 (2)
Ru(2)	−0.16839 (5)	0.23432 (4)	0.02899 (3)	3.53 (1)	C(1364)	0.6125 (7)	0.1552 (8)	0.6525 (5)	5.9 (3)
N(111)	0.2535 (5)	0.0963 (4)	0.5544 (3)	3.6 (1)	C(1365)	0.6569 (8)	0.1162 (7)	0.5959 (6)	6.0 (3)
N(121)	0.4533 (5)	0.3596 (4)	0.5615 (4)	3.9 (2)	C(1366)	0.6156 (7)	0.1089 (7)	0.5299 (5)	5.4 (2)
N(131)	0.3913 (5)	0.1736 (4)	0.4579 (3)	3.2 (1)	C(222′)	−0.2640 (8)	0.2736 (7)	−0.1017 (5)	5.7 (2)
N(211)	−0.2522 (5)	0.0995 (4)	−0.0272 (3)	3.7 (1)	C(223′)	−0.2882 (9)	0.3294 (7)	−0.1449 (6)	6.6 (3)
N(221)	−0.0932 (5)	0.3705 (5)	0.0781 (4)	4.1 (2)	C(224′)	−0.2566 (8)	0.4248 (8)	−0.1229 (6)	6.9 (3)
N(231)	−0.1323 (5)	0.1764 (4)	0.1029 (3)	3.7 (1)	C(225′)	−0.1989 (7)	0.4635 (6)	−0.0598 (6)	5.8 (2)
N(121′)	0.3098 (5)	0.3034 (5)	0.6436 (4)	4.2 (2)	C(226′)	−0.1731 (6)	0.4054 (5)	−0.0187 (4)	4.1 (2)
N(1322)	0.2410 (5)	0.2577 (4)	0.4873 (3)	3.7 (1)	C(2321)	0.0075 (6)	0.1496 (5)	0.0381 (4)	3.7 (2)
N(1362)	0.4807 (5)	0.1811 (4)	0.5783 (3)	3.8 (1)	C(2323)	0.0148 (7)	0.2082 (6)	−0.0626 (5)	4.8 (2)
N(221′)	−0.2058 (5)	0.3100 (5)	−0.0412 (3)	4.1 (2)	C(2324)	0.1036 (7)	0.1752 (8)	−0.0807 (5)	5.8 (3)
N(2322)	−0.0324 (5)	0.1969 (4)	−0.0046 (3)	3.7 (1)	C(2325)	0.1439 (7)	0.1296 (7)	−0.0377 (6)	5.8 (2)
N(2362)	−0.2870 (5)	0.2515 (4)	0.0921 (4)	4.0 (2)	C(2326)	0.0973 (7)	0.1166 (6)	0.0215 (5)	5.0 (2)
C(112)	0.1811 (7)	0.0431 (6)	0.5025 (4)	4.3 (2)	C(2361)	−0.2799 (7)	0.2207 (6)	0.1510 (4)	4.2 (2)
C(113)	0.1216 (8)	−0.0440 (7)	0.5053 (5)	5.6 (2)	C(2363)	−0.3650 (7)	0.2967 (6)	0.0843 (6)	5.3 (2)
C(114)	0.1333 (9)	−0.0794 (7)	0.5629 (6)	6.4 (3)	C(2364)	−0.4350 (7)	0.3093 (7)	0.1323 (6)	5.5 (2)
C(115)	0.2064 (8)	−0.0254 (7)	0.6159 (5)	5.4 (2)	C(2365)	−0.4279 (8)	0.2756 (7)	0.1913 (6)	5.9 (3)
C(116)	0.2647 (7)	0.0615 (7)	0.6108 (5)	4.8 (2)	C(2366)	−0.3506 (7)	0.2302 (7)	0.2005 (5)	5.1 (2)
C(122)	0.5298 (7)	0.3819 (6)	0.5218 (5)	5.0 (2)	P(1000)	0.4303 (2)	0.0928 (2)	0.8250 (1)	5.93 (7)
C(123)	0.6041 (8)	0.4675 (7)	0.5371 (6)	5.8 (3)	P(2000)	−0.2326 (3)	0.3327 (3)	0.3928 (2)	8.5 (1)
C(124)	0.5973 (9)	0.5330 (8)	0.5962 (7)	7.0 (3)	P(3000)	0.2595 (2)	0.3296 (2)	0.1929 (2)	5.54 (6)
C(125)	0.5183 (9)	0.5126 (7)	0.6382 (6)	6.6 (3)	P(4000)	0.0683 (3)	−0.0909 (2)	0.2792 (1)	6.32 (7)
C(126)	0.4461 (7)	0.4255 (6)	0.6195 (5)	4.7 (2)	F(1001)	0.3867 (6)	0.0291 (6)	0.7508 (4)	9.8 (2)
C(132)	0.3359 (7)	0.1762 (5)	0.4016 (4)	3.9 (2)	F(1002)	0.4254 (9)	0.0011 (6)	0.8507 (5)	12.7 (3)
C(133)	0.3634 (8)	0.1419 (7)	0.3359 (5)	5.2 (2)	F(1003)	0.5448 (6)	0.0905 (7)	0.8034 (5)	11.3 (3)
C(134)	0.4486 (8)	0.1032 (7)	0.3302 (5)	5.8 (2)	F(1004)	0.441 (1)	0.1832 (6)	0.7961 (5)	14.0 (4)
C(135)	0.5054 (8)	0.1006 (7)	0.3888 (5)	5.2 (2)	F(1005)	0.3198 (7)	0.0911 (9)	0.8471 (6)	14.8 (4)
C(136)	0.4753 (7)	0.1359 (5)	0.4532 (4)	3.9 (2)	F(1006)	0.4786 (8)	0.1557 (7)	0.8984 (4)	11.3 (3)
C(212)	−0.3257 (7)	0.0439 (6)	0.0004 (5)	4.8 (2)	F(2001)	−0.3457 (7)	0.3349 (7)	0.3687 (5)	11.1 (3)
C(213)	−0.3804 (8)	−0.0457 (7)	−0.0343 (6)	6.0 (3)	F(2002)	−0.1942 (8)	0.3570 (7)	0.3232 (5)	11.7 (3)
C(214)	−0.3579 (8)	−0.0802 (7)	−0.1013 (6)	6.4 (3)	F(2003)	−0.2616 (8)	0.2223 (6)	0.3564 (5)	11.9 (3)
C(215)	−0.2817 (8)	−0.0247 (7)	−0.1298 (6)	5.9 (3)	F(2004)	−0.2775 (8)	0.3067 (8)	0.4629 (4)	12.5 (3)
C(216)	−0.2309 (7)	0.0644 (6)	−0.0921 (5)	4.6 (2)	F(2005)	−0.2098 (9)	0.4410 (8)	0.4295 (6)	15.1 (4)
C(222)	−0.0353 (7)	0.3969 (6)	0.1396 (5)	4.9 (2)	F(2006)	−0.1243 (7)	0.326 (1)	0.4169 (7)	18.2 (5)
C(223)	0.0038 (9)	0.4885 (7)	0.1735 (6)	6.2 (3)	F(3001)	0.3334 (6)	0.3034 (5)	0.2455 (4)	10.5 (2)
C(224)	−0.0196 (8)	0.5587 (7)	0.1447 (6)	6.3 (3)	F(3002)	0.3073 (8)	0.2737 (8)	0.1283 (5)	13.5 (3)
C(225)	−0.0766 (7)	0.5343 (6)	0.0818 (6)	5.6 (2)	F(3003)	0.3512 (8)	0.4151 (6)	0.1883 (6)	14.1 (3)
C(226)	−0.1135 (6)	0.4391 (6)	0.0478 (5)	4.2 (2)	F(3004)	0.2210 (9)	0.3882 (9)	0.2513 (6)	18.8 (4)
C(232)	−0.0483 (6)	0.1387 (5)	0.0989 (4)	3.8 (2)	F(3005)	0.1795 (8)	0.2384 (7)	0.1921 (5)	15.3 (3)
C(233)	−0.0230 (7)	0.0968 (6)	0.1504 (5)	5.0 (2)	F(3006)	0.1863 (6)	0.3525 (6)	0.1369 (4)	9.6 (2)
C(234)	−0.0843 (8)	0.0947 (7)	0.2057 (5)	5.9 (2)	F(4001)	0.048 (1)	−0.1454 (6)	0.3383 (4)	15.7 (4)
C(235)	−0.1716 (8)	0.1343 (7)	0.2098 (5)	5.5 (2)	F(4002)	0.047 (1)	−0.1877 (6)	0.2263 (5)	13.1 (3)
C(236)	−0.1923 (7)	0.1753 (6)	0.1557 (4)	4.2 (2)	F(4003)	−0.0525 (7)	−0.0971 (7)	0.2708 (6)	13.6 (3)
C(122′)	0.2296 (8)	0.2730 (7)	0.6796 (5)	5.4 (2)	F(4004)	0.076 (1)	0.0045 (7)	0.3319 (6)	17.2 (5)
C(123′)	0.1969 (9)	0.333 (1)	0.7343 (6)	8.2 (3)	F(4005)	0.1830 (7)	−0.0810 (8)	0.2909 (7)	20.2 (4)
C(124′)	0.251 (1)	0.425 (1)	0.7517 (8)	11.3 (4)	F(4006)	0.0829 (6)	−0.0371 (5)	0.2204 (4)	10.0 (2)
C(125′)	0.330 (1)	0.4593 (9)	0.7151 (7)	8.9 (4)	O(5000)	0.375 (2)	0.350 (2)	−0.022 (1)	23.1 (8)*
C(126′)	0.3609 (7)	0.3964 (7)	0.6616 (5)	5.1 (2)	O(6000)	0.174 (2)	0.635 (2)	0.327 (1)	25 (1)*
C(1321)	0.2489 (7)	0.2230 (6)	0.4180 (4)	4.2 (2)	C(5000)	0.381 (2)	0.412 (1)	0.927 (1)	12.0 (5)*
C(1323)	0.1681 (7)	0.3037 (7)	0.5055 (5)	5.1 (2)	C(5001)	0.341 (2)	0.479 (1)	0.933 (1)	12.1 (5)*
C(1324)	0.0987 (8)	0.3176 (7)	0.4587 (6)	6.4 (3)	C(5002)	0.470 (2)	0.416 (2)	0.879 (1)	13.5 (6)*
C(1325)	0.1032 (8)	0.2810 (7)	0.3892 (6)	6.3 (3)	C(6001)	0.020 (3)	0.632 (2)	0.375 (2)	20 (1)*
C(1326)	0.1790 (7)	0.2333 (6)	0.3680 (5)	4.9 (2)	C(6002)	0.113 (4)	0.650 (4)	0.380 (3)	31 (2)*
C(1361)	0.5273 (6)	0.1411 (6)	0.5219 (5)	4.3 (2)	C(6003)	0.106 (3)	0.524 (2)	0.380 (2)	21 (1)*

[a] Starred values denote atoms that were refined isotropically. Values for anisotropically refined atoms are given in the form of the isotropic equivalent thermal parameter defined as: $(4/3)[a^2\beta(1,1) + b^2\beta(2,2) + c^2\beta(3,3) + ab(\cos\gamma)\beta(1,2) + ac(\cos\beta)\beta(1,3) + bc(\cos\alpha)\beta(2,3)]$.

Some of the distances and angles are of particular interest. The longest Ru–N bond occurs to the pyridine ligand, and the shortest Ru–N bond occurs to the central nitrogen of the trpy ligand. This bond is about 0.1 Å shorter than the Ru–N bonds to the terminal nitrogens of trpy, consistent with the strain intrinsic to the metal–terpyridine moiety.[22-24] The N–Ru–N angle of about 159° formed by the terminal terpyridine nitrogens is also typical.[24] The bipyridine ligand is coordinated in an asymmetric fashion, and the longer Ru–N bond is associated with the nitrogen that is cis to the pyridine ligand. As can be appreciated from the data in Table V, the pyridine ligand is roughly perpendicular to the plane of the trpy ligand, but it is rotated 115–120° relative to the bpy ligand.

Discussion

Structure of $[Ru(trpy)(bpy)(py)]^{2+}$. The coordination sphere of $[Ru(trpy)(bpy)(py)]^{2+}$ is crowded and shows obvious signs of interligand steric interactions. The difference between the two Ru–N bond lengths of the bpy ligand is almost 0.04 Å, with the longer bond occurring to the bpy nitrogen that is cis to the py nitrogen and trans to the central nitrogen of the trpy ligand. The Ru–N bond length to the other nitrogen of the bpy can be considered normal as it is, within experimental error, equal to the Ru–N bond length (2.056 (6) Å) observed in $[Ru(bpy)_3](PF_6)_2$.[25]

(22) Figgis, B. N.; Kucharski, E. S.; White, A. H. *Aust. J. Chem.* **1983**, *36*, 1563–1571.
(23) Thummel, R. P.; Jahng, Y. *Inorg. Chem.* **1986**, *25*, 2527–2534.
(24) Leising, R. A.; Kubow, S. A.; Churchill, M. R.; Buttrey, L. A.; Ziller, J. W.; Takeuchi, K. J. *Inorg. Chem.* **1990**, *29*, 1306–1312.
(25) Rillema, D. P.; Jones, D. S.; Levy, H. A. *J. Chem. Soc., Chem. Commun.* **1979**, 849–851.

Table V. Selected Bond Distances (Å) and Angles (deg) for $[Ru(trpy)(bpy)(py)]^{2+}$

Formula Unit 1			
Distances			
N(1322)-Ru(1)	2.078 (7)	N(121)-Ru(1)	2.060 (6)
N(131)-Ru(1)	1.963 (6)	N(121')-Ru(1)	2.097 (7)
N(1362)-Ru(1)	2.079 (7)	N(111)-Ru(1)	2.114 (6)
Angles			
N(1322)-Ru(1)-N(1362)	159.3 (3)	N(1362)-Ru(1)-N(111)	89.1 (3)
N(1322)-Ru(1)-N(131)	79.7 (3)	N(131)-Ru(1)-N(121)	95.7 (3)
N(1322)-Ru(1)-N(121)	93.4 (3)	N(131)-Ru(1)-N(121')	171.9 (3)
N(1322)-Ru(1)-N(121')	94.8 (3)	N(131)-Ru(1)-N(111)	91.0 (2)
N(1322)-Ru(1)-N(111)	92.6 (2)	N(121)-Ru(1)-N(121')	78.7 (3)
N(1362)-Ru(1)-N(131)	79.7 (3)	N(121)-Ru(1)-N(111)	171.8 (3)
N(1362)-Ru(1)-N(121)	87.3 (3)	N(121')-Ru(1)-N(111)	95.2 (3)
N(1362)-Ru(1)-N(121')	105.5 (3)		
Formula Unit 2			
Distances			
N(2322)-Ru(2)	2.078 (7)	N(221)-Ru(2)	2.047 (7)
N(231)-Ru(2)	1.955 (7)	N(221')-Ru(2)	2.087 (7)
N(2362)-Ru(2)	2.052 (7)	N(211)-Ru(2)	2.100 (6)
Angles			
N(2322)-Ru(2)-N(2362)	158.7 (3)	N(2362)-Ru(2)-N(211)	93.1 (3)
N(2322)-Ru(2)-N(231)	79.1 (3)	N(231)-Ru(2)-N(221)	96.1 (3)
N(2322)-Ru(2)-N(221)	94.5 (3)	N(231)-Ru(2)-N(221')	173.5 (3)
N(2322)-Ru(2)-N(221')	104.2 (3)	N(231)-Ru(2)-N(211)	88.7 (3)
N(2322)-Ru(2)-N(211)	87.6 (3)	N(221)-Ru(2)-N(221')	78.2 (3)
N(2362)-Ru(2)-N(231)	79.6 (3)	N(221)-Ru(2)-N(211)	175.1 (3)
N(2362)-Ru(2)-N(221)	86.6 (3)	N(221')-Ru(2)-N(211)	97.0 (3)
N(2362)-Ru(2)-N(221')	96.9 (3)		
Dihedral Angles between Pyridine Moieties[a]			
Formula Unit 1			
N(131)-N(121')	93.13 (0.33)	N(121')-N(111)	114.79 (0.31)
N(131)-N(111)	90.27 (0.28)		
Formula Unit 2			
N(231)-N(221')	99.61 (0.30)	N(221')-N(211)	120.26 (0.27)
N(231)-N(211)	84.36 (0.28)		

[a] Pyridine moiety specified by the nitrogen atom contained therein.

The long Ru–N bond to bpy is unlikely to be due to a trans effect associated with the opposite nitrogen of the trpy ligand because no elongation occurs in another known mixed-ligand complex involving terpyridine and ruthenium(II).[24] On the contrary, the long Ru–N bond to bpy can be ascribed to a steric clash between the bpy and the py ligands. Similar steric crowding apparently occurs in $[Ru(bpy)_2(py)_2]^{2+}$. In the crystalline state, the latter complex exhibits Ru–N bonds to py of lengths 2.06 (3) and 2.13 (3) Å.[26] Furthermore, one of the bpy ligands is coordinated in a very asymmetric fashion with one Ru–N bond length of 2.13 (2) and one of 2.04 (3) Å. Here too, the two long Ru–N bonds are in a cis arrangement. The steric congestion can be expected to be even worse in $[Ru(trpy)(bpy)(2\text{-Me-py})]^{2+}$, and this probably explains the problems encountered in the synthesis of this derivative.

Absorption Spectra. Some consideration of the absorption spectra is in order as these data are important in the interpretation of the photosubstitution studies. As noted above, the most intense visible absorption band of the $[Ru(trpy)(bpy)L]^{2+}$ derivatives is attributable to unresolved charge-transfer transitions from the metal center to the π^* orbitals of the trpy and bpy ligand systems. When the nitrile ligand is replaced with a stronger donor such as pyridine, these bands exhibit a red shift due to the inductive effect.

Because pyridine is a smaller ring system with a higher energy π^* orbital, the band at 415 nm in the spectrum of the pyridine complex can be assigned as Ru(II) → py charge transfer. In accord with this assignment, the intensity of the absorption is enhanced in the case of the 4-Ph-py derivative due to conjugation of the aryl substituent.[27] In the case of the 2-Me-py derivative, the Ru → py CT band is poorly resolved, and here the red shifts

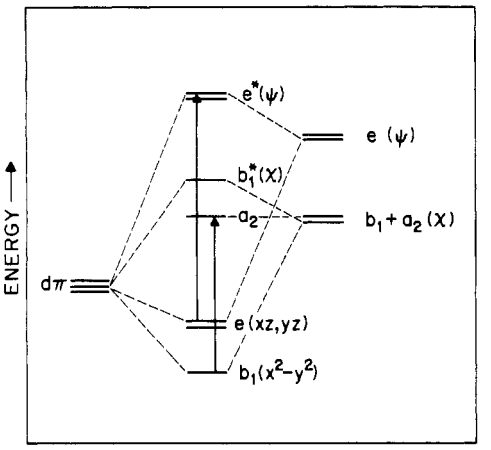

Figure 7. Schematic one-electron energy-level diagram for $[Ru(trpy)_2]^{2+}$ in D_{2d} symmetry. The x, y, and z axes are chosen to lie along the C_2 symmetry elements aligned so that the z axis passes through each ligand. Arrows indicate the z-polarized transitions.

in the transitions to the bpy and trpy ligands are smaller as well. These results can be explained in terms of the increase in the interligand steric repulsions, which are expected to lead to a longer ruthenium to nitrogen bond for the 2-Me-py ligand.

One explanation for the low-energy shoulders in the absorption spectra can be couched in terms of the qualitative orbital splitting diagram for $[Ru(trpy)_2]^{2+}$ in Figure 7. As with $[Ru(bpy)_3]^{2+}$, the relative energies of the molecular orbitals can be inferred from the zero-order energies of the ligand orbitals.[28] The two lowest lying π^* orbitals of the trpy ligand are labeled in light of their symmetry with respect to the plane of symmetry, which is perpendicular to the ligand and passes through the central nitrogen. An AM1 calculation[29,30] reveals that the lowest energy unoccupied orbital, termed χ, is antisymmetric with respect to this operation. It lies 0.453 eV below the next lowest energy π^* orbital, termed ψ, which is symmetric with respect to the reflection operator. Under the assumption of D_{2d} symmetry, the χ orbitals from the trpy ligand span the a_2 and the b_1 representations while the higher energy ψ orbitals span the e representation. Simple perturbation theory arguments and overlap considerations lead to the orbital splitting scheme in Figure 7.

In accordance with the theory developed by Mulliken,[31,32] the transitions with significant oscillator strength should be those that are z polarized, and they are indicated in Figure 7. What should be the lowest energy transition, namely the e → a_2 orbital excitation, is allowed, but it occurs with xy polarization and should be comparatively weak since it does not benefit from the charge-transfer term.[31] This restriction is relaxed in a lower symmetry complex such as $[Ru(trpy)(bpy)(NCCH_3)]^{2+}$, but qualitatively similar results can be expected. Thus, one or more of the low-energy shoulders of the absorption spectra in Figure 1 may be due to weak, orbitally allowed charge-transfer transitions. Transitions to low-energy triplet states may also occur,[33,34] especially in the osmium analogues.

Photochemistry. Key steps in the model invoked to explain the photochemistry of ruthenium(II) complexes of polypyridine ligands are outlined in eqs 1–5. In this scheme ^{3}CT denotes a vibrationally

(26) Hitchcock, P. B.; Seddon, K. R.; Turp, J. E.; Yousif, Y. Z.; Zora, J. A.; Constable, E. C.; Wernberg, O. *J. Chem. Soc., Dalton Trans.* **1988**, 1837–1842.
(27) Phifer, C. C.; McMillin, D. R. *Inorg. Chem.* **1986**, *25*, 1329–1333.
(28) Ceulemans, A.; Vanquickenborne, L. G. *J. Am. Chem. Soc.* **1981**, *103*, 2238–2241.
(29) Dewar, M. J. S.; Zoebisch, E. G.; Healy, E. F.; Stewart, J. J. P. *J. Am. Chem. Soc.* **1985**, *107*, 3902–3909.
(30) Calculations were performed on a Silicon Graphics 4D-25 computer using MOPAC version 5.0, obtained from James P. Stewart and Frank J. Seiler of the USAF Academy, Colorado Springs, CO. The coordinates for the atoms of trpy were taken from Table IV.
(31) Mulliken, R. S. *J. Am. Chem. Soc.* **1952**, *74*, 811–824.
(32) Day, P.; Sanders, N. *J. Chem. Soc. A* **1967**, 1536–1541.
(33) Kober, E. M.; Meyer, T. J. *Inorg. Chem.* **1982**, *21*, 3967–3977.
(34) Yersin, H.; Braun, D.; Hensler, G.; Gallhuber, E. In *Vibronic Processes in Inorganic Chemistry*; Flint, C. D., Ed.; Kluwer: Boston, MA, 1989; pp 195–219.

$$^3CT \underset{k_{-1}}{\overset{k_1}{\rightleftharpoons}} {}^*Ru\text{–}L \quad (1)$$

$$^*Ru\text{–}L \xrightarrow{k_2} Ru\text{–}L \quad (2)$$

$$^*Ru\text{–}L \xrightarrow{k_3} {}^*Ru + L \quad (3)$$

$$^*Ru \xrightarrow{k_4} Ru \quad (4)$$

$$Ru + X \xrightarrow{k_5} Ru\text{–}X \quad (5)$$

relaxed triplet charge-transfer excited state, *Ru–L denotes a ^{3}d–d excited state that is thermally accessible from ^{3}CT and prone to loss of ligand L, Ru–L denotes the ground-state complex, *Ru is the five-coordinate intermediate in a ^{3}d–d excited state, Ru is the same intermediate in its ground electronic state, X is a nucleophile, and Ru–X is a photoproduct. In this scheme, substitution occurs by way of a dissociative mechanism. The fact that the ^{3}CT state of the analogous osmium(II) derivative is effectively inert supports the notion that the ^{3}d–d state is involved, because the ^{3}d–d state is displaced to higher energy in the case of the third-row transition ion. A more complicated scheme is required if the five-coordinate intermediates can be intercepted by solvent or if ion-pairing equilibria occur with the nucleophile. However, most of the latter complications are avoided in our system. Clearly, ion-pairing equilibria can be ignored since neutral pyridine derivatives are used as the nucleophiles. Furthermore, the leaving group is acetonitrile so that attack of the five-coordinate intermediate Ru by solvent simply regenerates the starting material.

Consistent with a purely dissociative process, virtually identical results are obtained with the py and the 4-Ph-py systems. More striking is the fact that a significantly higher quantum yield is observed with 2-Me-py as the nucleophile. The 2-Me-py ligand is so bulky that this result simply cannot be reconciled with an associative process. A possible explanation within the context of a dissociative mechanism is that the nitrogen center of 2-Me-py may be more weakly solvated than those of the other pyridines and that this favors attack of the five-coordinate intermediate (eq 5).

We cannot rule out the possibility that pyridine reacts with a high-energy isomer of the ground state such an η^2, or side-on, adduct of acetonitrile or an intermediate with the solvent coordinated to the metal center via a C–H bond.[35] However, even if an unstable isomer of this type is involved in the reaction, the inference that the primary process is a dissociative one still seems secure. The reason is that this kind of isomer would most plausibly be formed by dissociation followed by recombination.

Although the *net* photochemistry that occurs is quite simple, other nonproductive processes may also be involved, because population of the $d_{x^2-y^2}$ or the d_{z^2} orbital tends to labilize multiple ligands.[36] Indeed, success has been achieved in rationalizing the product yields and product stereochemistry in d^6 systems from theoretical estimates of the metal-to-ligand bond strengths in the excited state.[37] Because of the short bond to the central nitrogen of the terpyridine ligand, the energies of the d orbitals involved in σ antibonding interactions are expected to be[38]

$$d_{x^2-y^2} < d_{z^2} \quad (6)$$

where the z axis is assumed to fall along the Ru–N(131) bond in Figure 6. Bonds to all ligands in the xy plane are likely to be weakened in the lowest energy ^{3}d–d state; hence, dissociation of a bpy nitrogen, an outer pyridine nitrogen of the trpy ligand, or acetonitrile is possible.

In an attempt to detect competing reactions, we irradiated $[Ru(trpy)(bpy)(NCCH_3)]^{2+}$ in the presence of ca. 1 M bpy ligand. A comparison of Figures 3 and 4 reveal that a qualitatively different product spectrum develops when the entering group is a potential chelating ligand. In particular, in Figure 4, the absorbance uniformly increases between 350 and 500 nm. Furthermore, the difference spectrum indicates that the shoulder which appears at ca. 570 nm in the absorption spectrum of $[Ru(trpy)(bpy)(NCCH_2)]^{2+}$ tends to be lost instead of red shifted in the photoproduct. Formation of $[Ru(\eta^2\text{-trpy})(bpy)_2]^{2+}$, where the trpy ligand acts as a bidentate ligand, is the obvious process that could explain an overall absorbance increase and modification of the ruthenium terpyridine chromophore. Photoinduced formation of an η^2-terpyridine complex has a precedent in ruthenium chemistry.[19] Photodissociation of a terminal nitrogen of trpy, attack by bpy to give an η^1 adduct, and then ring closure with loss of the acetonitrile ligand would give the proposed product. Alternatively, the same product could be obtained by photodetachment of the acetonitrile group if chelation of bpy occurs with conversion to η^2-trpy. In view of this ambiguity, we made no attempt to analyze the reaction further. Although we have not measured the product yield, it is possible that the quantum efficiency is reduced when bpy is the nucleophile. This could happen if the putative η^1-bpy intermediate is sufficiently strained that the monodentate bpy is efficiently deligated via a secondary photochemical process of some type of competing thermal process.

Luminescence Decay Rates. Equation 7, first used by Allsopp et al.,[39] adequately describes the temperature-dependent decay of the excited states of ruthenium(II) systems unless a phase

$$\frac{1}{\tau(T)} = k_0 + \sum A_i \exp[-\Delta E_i/(RT)] \quad (7)$$

change of the matrix perturbs the system significantly. When matrix effects intervene, additional terms must be used.[40] In this equation, k_0 is the sum of the radiative and nonradiative decay rate constants, which exhibit no temperature dependence in the range of interest. Beyond this, two types of Arrhenius terms are often required to fit the data. The term with the higher ΔE (>1000 cm^{-1}) usually has the higher frequency factor too ($>10^{12}$ s^{-1}). In Table II, the convention is to assign subscript 1 to the high-barrier process and subscript 2 to the low-barrier process.

The ΔE_1 value is usually regarded as the barrier to internal conversion to a nearby ^{3}d–d excited state.[40,41] On the other hand, the ΔE_2 process represents relaxation via another ^{3}CT excited state.[41] As can be seen in Figure 5A, the emission maximum shifts to longer wavelengths at higher temperatures in the nitrile solvent system. This probably reflects solvent relaxation at the higher temperatures; nevertheless, only the ΔE_1 process could be resolved from the lifetime data (Table II). The influence the solvation changes have on the lifetime are evidently obscured by the early onset of relaxation via the ^{3}d–d state. The fact that the latter process has a very modest barrier explains why relatively efficient photochemistry is observed. A similar barrier ($\Delta E_1 \sim 1500$ cm^{-1}) has been observed for $[Ru(trpy)_2]^{2+}$ in an alcohol glass;[42] however, hardly any net photochemistry can be detected from this ion. These apparently contradictory results can be explained by the fact that dissociation of a metal–ligand bond in $[Ru(trpy)_2]^{2+}$ leads to an η^2-trpy derivative for which ring closure to the η^3 form is undoubtedly quite efficient.[19]

Results obtained in the polymer matrix are also listed in Table II, and here there is no evidence of a ΔE_1 term. This probably indicates that the ^{3}d–d state is less accessible in the rigid polymer matrix. The alternative interpretation is that the ^{3}d–d state and the emissive charge-transfer state are actually in equilibrium in the polymer matrix. This could conceivably be the case in a rigid matrix if ligand dissociation and deactivation of the ^{3}d–d state are inhibited. In this event, the ΔE_2 term can no longer be considered an activation energy; instead, it corresponds to an internal energy.[43] For the moment we cannot distinguish between

(35) Xie, X. L.; Simon, J. D. *J. Am. Chem. Soc.* **1990**, *112*, 1130–1136.
(36) Zink, J. I. *Inorg. Chem.* **1973**, *12*, 1018–1024.
(37) Vanquickenborne, L. G.; Ceulemans, A. *Coord. Chem. Rev.* **1983**, *48*, 157–202.
(38) Figgis, B. N.; Kucharski, E. S.; White, A. H. *Aust. J. Chem.* **1983**, *36*, 1537–1561.
(39) Allsopp, S. R.; Cox, A.; Kemp, T. J.; Reed, W. R. *J. Chem. Soc., Faraday Trans. I* **1978**, *74*, 1275–1289.
(40) Barigeletti, F.; Juris, A.; Balzani, V.; Belser, P.; von Zelewsky, A. *J. Phys. Chem.* **1987**, *91*, 1095–1098.
(41) Lumpkin, R. S.; Kober, E. M.; Worl, L. A.; Murtaza, Z.; Meyer, T. J. *J. Phys. Chem.* **1990**, *94*, 239–243.
(42) Lytle, F. E.; Hercules, D. M. *J. Am. Chem. Soc.* **1969**, *91*, 253–257.

the two interpretations. However, since ΔE_1 and ΔE_2 processes are observed in the crystalline state where dissociation is also likely to be hindered, we suspect that in the polymer matrix the ^{3}d-d state is simply not accessed in the temperature range investigated.

Conclusions

Photolysis of $[Ru(trpy)(bpy)(NCCH_3)]^{2+}$ dissolved in acetonitrile solutions containing various pyridine derivatives leads to substitution of the acetonitrile ligand by the pyridine. A quantum yield of about 0.0013 can be measured for pyridine and 4-phenylpyridine, while for the sterically hindered 2-methylpyridine the quantum yield is increased approximately 2-fold. These results are incompatible with an associative mechanism of substitution, but they can be reconciled with a dissociative mechanism. In the case of 2-methylpyridine, the increase in quantum yield may reflect a difference in solvation of the entering nucleophile. Previous evidence for a dissociative mechanism in the photosubstitution chemistry of a ruthenium(II) polypyridine complex is available from studies of the photoanation of $[Ru(bpy)_2(py)_2]^{2+}$ in methylene chloride, where the quantum yield for replacement of the first pyridine was found to be independent of the anion.[44] The quantum yields for substitution are low for $[Ru(trpy)(bpy)(NCCH_3)]^{2+}$ despite the fact that the temperature dependence of the luminescence lifetime reveals that there is only a modest barrier (ca. 1500 cm^{-1}) separating the emissive ^{3}CT state from the reactive ^{3}d-d state. Undoubtedly, the yields are attenuated by the fact that the solvent competes for the empty coordination site of the putative five-coordinate intermediate. In addition, dissociation of a terminal Ru-N bond of the trpy and/or bpy ligand in place of the acetonitrile ligand would be expected to lead to no net reaction, since ring closure and regeneration of the original complex is highly favored. Finally, the product complex $[Ru(trpy)(bpy)(py)]^{2+}$ has been structurally characterized as the PF_6^- salt by X-ray crystallography. There is evidence for steric strain in the coordination sphere of ruthenium in the form of a long bond to the pyridine nitrogen and asymmetric coordination of the bpy ligand.

Acknowledgment. This research was supported by NSF Grant No. CHE-8719538. We are indebted to Dan Severance, who did most of the work involved with the AM1 calculation.

Supplementary Material Available: For $[Ru(trpy)(bpy)(py)](PF_6)_2 \cdot (CH_3)_2CO$, tables listing positional parameters and their estimated standard deviations, general temperature factor expressions, bond distances, and bond angles, torsion angles, and least-squares planes along with their dihedral angles (36 pages); a table of calculated and observed structure factors (26 pages). Ordering information is given on any current masthead page.

(43) Juris, A.; Balzani, V.; Barigelletti, F.; Campagna, S.; Belser, P.; von Zelewsky, A. *Coord. Chem. Rev.* **1988**, *84*, 85-277.
(44) Durham, B.; Walsh, J. L.; Carter, C. L.; Meyer, T. J. *Inorg. Chem.* **1980**, *19*, 860-865.

Contribution from the Department of Chemistry, Frick Laboratory, Princeton University, Princeton, New Jersey 08544-1009

Surface-Attached $[(NC)_5Fe(CN)Pt(NH_3)_4(NC)Fe(CN)_5]^{4-}$: A Study in the Electrochemical and Photochemical Control of Surface Morphology

Brian W. Pfennig and Andrew B. Bocarsly*

Received July 3, 1990

The $[Pt(NH_3)_4]_2^{4+}$ salt of $[(NC)_5Fe^{II}(CN)Pt^{IV}(NH_3)_4(NC)Fe^{II}(CN)_5]^{4-}$ (I) was electrochemically derivatized on a Ni surface by anodic precipitation as the Ni^{2+} analogue, Ni_2I. The resulting electrode surface was characterized by diffuse-reflectance FTIR spectroscopy and cyclic voltammetry. The cyclic voltammetric response of this species was similar to that of the solution species and was found to be only slightly variant with intercalated cation. However, this noncrystalline surface could be photochemically modified to generate a nickel ferrocyanide lattice, which is electrochemically cation sensitive. The photoinduced crystallization process was monitored by parallel electrochemical and X-ray powder pattern experiments. A mechanism for this transformation is proposed. In a separate set of reactions, it was found that the complex of interest can be electropolymerized onto an inert electrode surface. This process is believed to occur via oxidation of the "$[Fe^{II}Pt^{IV}Fe^{II}]^{4-}$" anion to form the "$[Fe^{III}Pt^{IV}Fe^{III}]^{2-}$" dianion, which in turn oxidizes one of the Pt(II) counterions to form the polymeric species "$[Fe^{II}Pt^{IV}]_n$." The spectroscopy and electrochemistry of the polymeric species is discussed.

Introduction

In the past several years, it has been demonstrated that electrochemical processes can be modulated and controlled by chemically modified electrodes.[1] Interest in our group has focused on the mixed-metal cyanometalate family of derivatized electrodes, which are structurally analogous with Prussian Blue. Typically, an anodically unstable metal electrode such as nickel is oxidized in the presence of a complex such as $Fe(CN)_5L^{2-}$. A precipitation reaction follows that leads to the formation of an ordered, cyanide-bridged lattice on the surface of the electrode.[1] We have shown that the charge transfer properties of these surface layers are closely related to the surface morphology. One simple technique for varying the surface structure and thus the electrochemical reactivity in the case of a nickel ferrocyanide surface lattice is to intercalate different alkali-metal cations. This process causes a shift in the surface iron redox potential of about 600 mV when Li^+ intercalation is compared with Cs^+ intercalation.[3,4] Our current focus is on designing and controlling the molecular architecture and therefore the microstructure of these three-dimensional lattices.

We have recently reported the single-crystal X-ray structure of the trinuclear, cyanide-bridged complex $\{[Pt(NH_3)_4]_2^{4+}\}\{[NC)_5Fe^{II}(CN)Pt^{IV}(NH_3)_4(NC)Fe^{II}(CN)_5]^{4-}\} \cdot 9H_2O$ ($[Pt(NH_3)_4]_2I$) shown in Figure 1.[5] This previously unreported complex was serendipitously discovered on an electrode surface while the potential of a nickel ferrocyanide derivatized electrode was cycled in a solution of tetraammineplatinum(II) nitrate and subsequently was prepared as a bulk material via reaction in solution. The $[Pt(NH_3)_4]_2I$ complex is interesting not only as it is a well-characterized molecular model of the nickel-cyanometalate system but also because it exhibits an optical intervalent

* Author to whom correspondence should be addressed.

(1) Bocarsly, A. B.; Sinha, S. *J. Electroanal. Chem. Interfacial Electrochem.* **1982**, *137*, 157 and references therein.
(2) Sinha, S.; Humphrey, B. D.; Bocarsly, A. B. *Inorg. Chem.* **1984**, *23*, 203.
(3) Bocarsly, A. B.; Sinha, S. *J. Electroanal. Chem. Interfacial Electrochem.* **1982**, *140*, 167.
(4) Amos, L. J.; Duggal, A.; Mirsky, E. J.; Ragonesi, P.; Bocarsly, A. B.; Fitzgerald-Bocarsly, P. A. *Anal. Chem.* **1988**, *60*, 245.
(5) Zhou, M.; Pfennig, B. W.; Steiger, J. L.; Van Engen, D.; Bocarsly, A. B. *Inorg. Chem.* **1990**, *29*, 2456.

0020-1669/91/1330-0666$02.50/0